A. Cuneyt Tas
Clemson University, Department of Materials Science and Engineering, Clemson, SC, USA

Electroless deposition of brushite ($CaHPO_4 \cdot 2\,H_2O$) crystals on Ti–6Al–4V at room temperature

Dedicated to Professor Dr. Fritz Aldinger on the occasion of his 65th birthday

An electroless, room temperature solution growth method of depositing 50 to 150 μm thick, well-crystallized brushite ($CaHPO_4 \cdot 2\,H_2O$, DCPD, dicalcium phosphate dihydrate) layers on the surface of an implantable medical device, such as a titanium alloy (Ti–6Al–4V) substrate, was developed. High ionic strength (189 to 609 mM) solutions with a Ca/P molar ratio of 2.50 and a pH value between 4.70 and 6.10 were prepared by dissolving appropriate quantities of $CaCl_2 \cdot 2\,H_2O$, NaH_2PO_4, $NaHCO_3$, and NaCl in deionized water. Surface-etched Ti–6Al–4V substrates were simply soaked in the solutions from 24 to 72 hours at room temperature. Elongated $CaHPO_4 \cdot 2\,H_2O$ crystals were in-situ-grown on the entire surfaces of the etched Ti–6Al–4V substrates.

Keywords: Titanium alloy; Calcium phosphate; Deposition; Brushite

1. Introduction

Ideally, orthopedic and dental biomedical devices, and particularly devices destined for in vivo implantation, must be perfectly compatible with the natural bone tissues. The ideal device should have a surface chemistry and biophysical structure so as to avoid an immune response to the presence of the device as well as to induce an osteogenic response similar to that of natural fracture healing upon its implantation. The ideal surface of an orthopedic implant should thus encourage initial invasion by mesenchymal stem cells, osteoclasts and osteoblasts, as well as exhibit osteoinduction leading to the complete osseointegration of the implant.

The mineral portion of the human bones and teeth is comprised of apatite-like calcium phosphate. Human bone mineral lacks a fixed composition, it is nonstoichiometric, and it can roughly be represented by the nominal formula $Ca_{10-x}(HPO_4)_x(PO_4)_{6-x}(CO_3{-}OH)_{1-x}$, where x ranges between 0 and 1 [1, 2]. Moreover, significant amounts of carbonate (5 wt.%), alkali and alkaline earth ions (such as, Na^+, K^+, Mg^{2+}; about 1.6 wt %), as well as trace elements, such as Zn, Fe, Cu, and Sr, are also found in biological apatites [3]. Human bone mineral contains protonated phosphate groups (i.e., HPO_4^{2-}) [4] and CO_3^{2-} ions, while significantly lacking the OH^- ions [5].

Synthetic calcium phosphates (CaP) lack the mechanical properties (flexural strength and toughness) of human bone mineral, and for that reason metallic implants are often used (e. g., Ti–6Al–4V for total hip replacement) for in vivo skeletal repair applications. Coating the surfaces of c. p. Ti or Ti–6Al–4V implants with CaP improve their bone-bonding ability [6]. Apatitic CaP can be coated on titanium and its alloys by using techniques as diverse as biomimetic coating [6], plasma spraying [7, 8], sputtering [9], and sol-gel dip-coating [10–12]. A number of researchers used electrochemical deposition processes in coating metallic surfaces with apatitic CaP [13–15]. Although apatitic CaP coatings impart osteoconductive (i. e., bone growing in opposition to the surface) properties to the metallic implant surfaces, hydroxyapatite-like coatings do not directly take part in the natural bone remodeling processes. To overcome this problem, some researchers used electrochemical deposition processes to coat more resorbable brushite ($CaHPO_4 \cdot 2\,H_2O$, DCPD, dicalcium phosphate dihydrate) on titanium substrates [16–22].

Brushite is a calcium phosphate phase of in vivo resorbability, despite its slight acidity [23]. Brushite has long been in successful clinical use in the powder formulations of CaP-based orthopedic cements [24, 25]. Relying on the experimental solubility values of some of the calcium phosphate phases recently reported by Tang et al. [26], brushite has a dissolution rate of 4.26×10^{-4} mol m^{-2} min^{-1} at a pH value of 5.5, and this rate is about 3.4 times greater than that of β-$Ca_3(PO_4)_2$ (i. e., 1.26×10^{-4}). To compare these numbers, the dissolution rate for carbonated apatite was reported by the same researchers to be 1.42×10^{-6} mol m^{-2} min^{-1} [26].

The motivation for this study can be briefly stated as follows; in the literature, there is yet no procedure described for the 3D growth of brushite on titanium alloy surfaces in aqueous solutions, without using electrochemical techniques. The current study presents, for the first time, a robust procedure for the electroless crystallization of brushite on Ti–6Al–4V substrates immersed into concentrated but optically transparent CaP solutions at room temperature. The solutions described here, in one sense, resemble synthetic body fluid (SBF) solutions [6, 27], but without pH adjustment at the physiological pH value of 7.4.

Table 1. Solution preparation recipes (1 l basis at RT).

	H_2O (ml)	NaCl (g)	$CaCl_2 \cdot 2\,H_2O$ (g)	NaH_2PO_4 (g)	$NaHCO_3$ (g)	Solution pH
Solution-1	980	–	8.086	2.639	0.2268	5.20
Solution-2	980	–	17.642	5.759	0.185	4.70
Solution-3	980	29.22	4.447	1.452	0.504	6.15

2. Experimental

2.1. Preparation of Ti–6Al–4V substrates

Rectangular samples (strips with dimensions of $10 \times 10 \times 0.35$ mm) were first cut from a Ti–6Al–4V sheet (Grade 5, ASTM B265, McMaster-Carr, Atlanta, GA), and then manually polished with a Grit 1200 SiC paper (Struers Inc., Cleveland, OH) to remove the thin scale layer present on the as-received titanium alloy sheet. Polished strips (or coupons) were washed three times with acetone, ethanol, and deionized water, respectively, in an ultrasonic bath for 30 min. Each one of the strips was then soaked in 75 ml of a 5M KOH solution at 60 °C for 24 h in a sealed 100 ml-capacity glass media bottle (Pyrex*Plus*®-Corning, Fisher Scientific, Pittsburgh, PA). Strips were then thoroughly rinsed with water in an ultrasonic bath, and stored at room temperature in 100 % humidity, sealed 1 l-capacity glass jars (i. e., a 25 ml plastic beaker, containing the strip, which was afloat in 900 ml of water present in the jar) until brushite was deposited.

2.2. Deposition solutions

Solutions prepared for the crystallization of brushite on Ti–6Al–4V substrates are described in Table 1. Solutions were prepared in 1.5 l glass beakers. First, 980 ml of deionized water were placed into these beakers. For Solution-1 and Solution-2, the first reagent added was $CaCl_2 \cdot 2\,H_2O$ (> 99 %, Fisher Scientific), and easily dissolved by stirring with a Teflon-coated stir-bar at room temperature (RT, 23 ± 1 °C). Secondly, NaH_2PO_4 (> 99 %, Fisher Scientific) was added and dissolved. However, for Solution-3, the first reagent added was NaCl (> 99 %, Fisher Scientific), followed by the respective additions of $CaCl_2 \cdot 2\,H_2O$ and NaH_2PO_4. All three solutions shown in Table 1 acquired a pH value in the range of 4.2 to 4.3, just prior to the addition of $NaHCO_3$.

Prior to the addition of $NaHCO_3$, these solutions (of pH 4.2 to 4.3) were extremely stable with respect to precipitation, and could even be stored in sealed glass containers at room temperature for more than a year without any turbidity being observed. After adding all reagents, the solution volume was completed to 1 l by adding deionized water. Further compositional characteristics of these solutions are given in Table 2. The way the ionic strength of these solutions was calculated has been demonstrated, only for Solution-3, by the calculation given at the bottom of Table 2. The relative supersaturation ratios for these brushite crystallization solutions were calculated by using the formula given in Table 2, where *IP* is the ionic product, K_{sp} is the solubility product (i. e., 2.32×10^{-7} for brushite at 25 °C), and ν is the total number of ions in the chemical formula of $CaHPO_4 \cdot 2\,H_2O$, so $\nu = 2$.

Four of the KOH-treated Ti–6Al–4V strips were placed to the bottom of a 1 l-capacity glass jar, and a 750 ml portion of the solution of interest was then gently poured into this glass jar, followed by sealing the jar. The jar was then simply kept undisturbed at RT. Every 24 h the solution in the jar was replaced with a fresh solution. Deposition was continued in this fashion from 24 to 72 h. During the crystallization period, there was also a very thin layer of white brushite precipitates accumulating at the bottom of the glass jars, apart from the strips. This is an environmentally-friendly process, and the used solutions can be discarded without any concerns or can be easily recycled back into the process. At the end of the deposition process, strips were white in appearance (indicating the complete coverage of the surfaces with brushite crystals), and were thoroughly washed with deionized water, followed by overnight drying at 37 °C in a laboratory oven.

2.3. Characterization

Phase analyses of the CaP crystals deposited on the Ti–6Al–4V strips were performed by using an X-ray diffractometer (XRD; XDS 2000, Scintag Corp., Sunnyvale, CA) operated with Cu K_α radiation at 40 kV and 30 mA, with a step size of 0.03° and preset time of 1 s at each step. The deposited substrates were placed directly on the sample holder of the X-ray diffractometer to determine the phase(s) present. Samples were also analyzed by using Fourier-transform infrared spectroscopy (FTIR; Nicolet 550, Thermo-Nicolet, Woburn, MA). Scanning electron microscopy (SEM; S-3500 and S-4700, Hitachi, Tokyo, Japan) was used in the secondary electron mode with an acceleration voltage of 5–15 kV to image the deposited CaP. Platinum sputtering was used to make the coating surfaces conductive for the SEM investigations. The thickness of the deposited brushite layers was directly evaluated from the SEM photomicrographs. Chemical analyses of the scraped (with a

Table 2. Compositional details of the solutions of Table 1.

	Solution-1	Solution-2	Solution-3
Ca^{2+} (mM)	55	120	30.25
$H_2PO_4^-$ (mM)	22	48	12.10
molar Ca/P	2.50	2.50	2.50
HCO_3^- (mM)	2.7	2.2	6
Na^+ (mM)	24.7	50.2	518.1
Cl^- (mM)	110	240	560.5
Ionic strength (mM)	189.7	410.2	609[a]
Rel. supersaturation (σ)	71.26	156.66	38.74[b]

[a] $I = {}^1/_2[(30.25 \times 10^{-3})\,(2)^2 + (12.1 \times 10^{-3})\,(1)^2 + (6 \times 10^{-3})\,(1)^2 + (518.1 \times 10^{-3})\,(1)^2 + (560.5 \times 10^{-3})\,(1)^2] = 0.609\,M$ (I = Ionic strength, M = molarity)

[b] σ = relative supersaturation ratio = $(IP/K_{sp})^{1/\nu} - 1$

sharp steel razor) deposits were performed by inductively coupled plasma atomic emission spectroscopy (ICP-AES; Model 61E, Thermo Jarrell Ash, Woburn, MA).

3. Results

The characteristic surface morphology of Ti–6Al–4V strips, which were soaked in hot 5 M KOH solutions for 24 h, is shown in Fig. 1. KOH solution etched the surface and created a nanoporous texture. The inset in Fig. 1 depicts the surface morphology at a higher magnification. All of the Ti–6Al–4V strips immersed in the deposition solutions of Tables 1 and 2 received the same treatment.

Early stages of brushite crystallization on KOH-treated Ti–6Al–4V strips were also monitored. The SEM micrograph given in Fig. 2 shows the bundles of brushite which were forming on the KOH-treated Ti–6Al–4V only surfaces after one hour of soaking in Solution-1 of Table 1. Other solutions of this study also formed similar bundles at the end of 1 h of soaking. As seen in Fig. 2, such bundles consisting of individual whiskers initially growing parallel to the surface, and then coalescing into a bundle shape were small in size and spatial extent at the beginning of this nucleation-growth process. The mid-points of those bundles seemed to facilitate the further growth of the individual whiskers (or crystals) typically in two opposing directions.

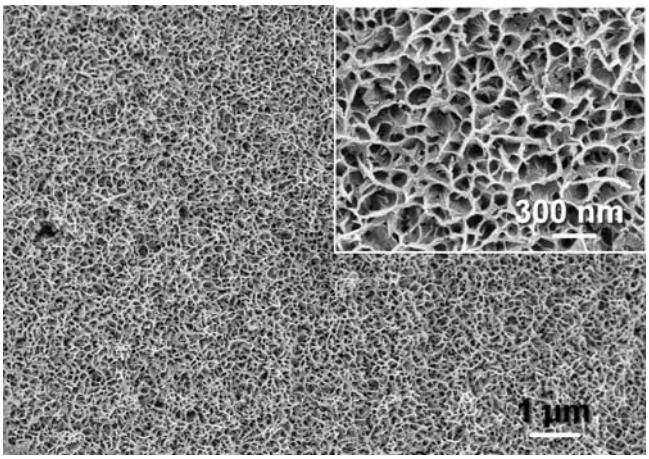

Fig. 1. Typical surface microstructure of neat Ti–6Al–4V substrates used in brushite deposition (after 24 h at 60 °C in 5 M KOH solution).

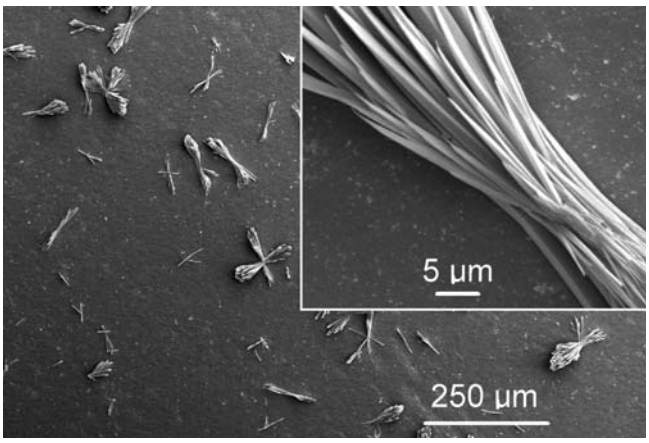

Fig. 2. Initial deposition of brushite crystal bundles on Ti–6Al–4V substrates (1 h in Solution-1 at RT).

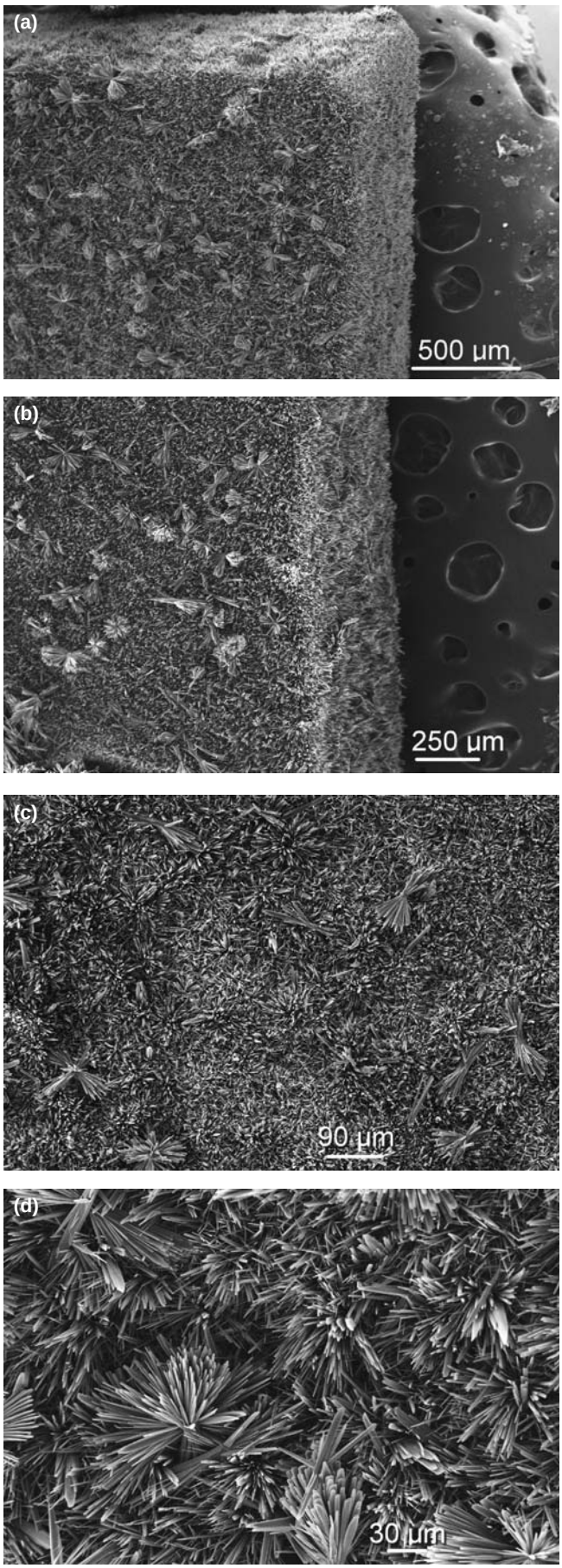

Fig. 3. Brushite deposition on Ti–6Al–4V substrates after soaking in Solution-2 for 48 h.

With an increase in time spent in the deposition solutions, CaP crystals grew more on Ti–6Al–4V strips, finally (after 36 to 48 h) covering in 3D all the available surface, with needles and bundles, as shown in the different magnification SEM micrographs of Fig. 3. Figures 3a and 3b also show the complete coverage of the sides of the strips, proving that this process was not simply a "physical-sedimentation-of-solution-crystals" onto the surfaces. The morphology of brushite grown on unetched Ti–6Al–4V substrates was similar to the ones obtained on the etched surfaces, but the amount of brushite formed on pristine surfaces was extremely low.

The characteristic XRD spectra of the crystals deposited on the Ti–6Al–4V surfaces is given in Fig. 4a. Crystals formed were single-phase brushite, $CaHPO_4 \cdot 2\,H_2O$. Crystallographic *hkl* indices of the brushite phase are shown for each peak in Fig. 4a. FTIR spectra (Fig. 4b) collected from the samples (taken either from the as-deposited Ti–6Al–4V strips or from the scraped-off powdery crystals) also confirmed the formation of single-phase brushite. XRD and FTIR data obtained from the coated strips did not change as a function of soaking time, meaning that there was no other transient or intermediate CaP phase(s) forming on the strips.

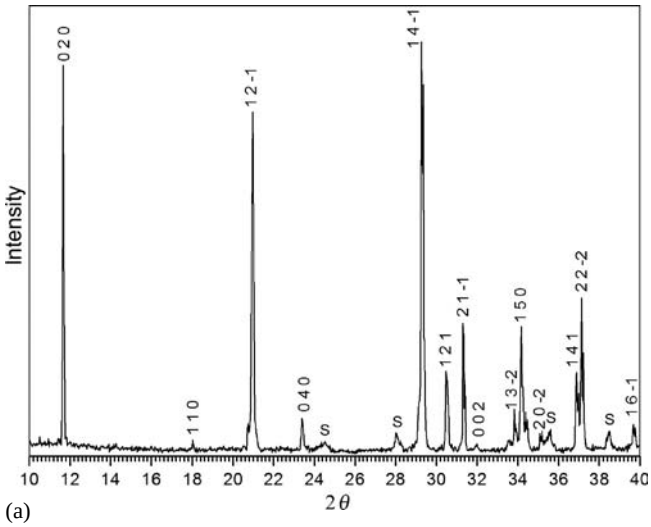

(a)

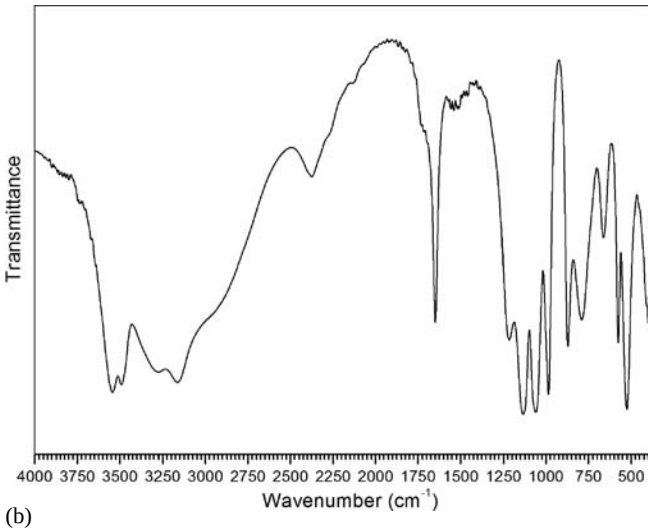

(b)

Fig. 4. XRD and FTIR spectra of Ti–6Al–4V substrates soaked in Solution-2 for 48 h (S: Ti–6Al–4V peaks).

More than forty solution recipes (for the brushite crystallization) have been developed throughout this study, and the solution recipes given in Table 1 are just selected examples. It should, therefore, be understood that changes in the Ca^{2+} and $H_2PO_4^-$ ion concentrations of those solutions, as well as those of HCO_3^-, would still be able to yield brushite crystallization. However, Solution-3 of Tables 1 and 2 is a unique recipe in the sense that it was able to simultaneously crystallize both brushite and apatitic CaP (or octacalcium phosphate), owing to its slightly higher pH value (i. e., 6.15). The SEM and optical micrographs of Figs. 5a and 5b reveal the formation of apatitic CaP spherulites (judged by their characteristic morphology) on the brushite crystals growing on the Ti–6Al–4V strips soaked in Solution-3 for 2 h.

4. Discussion

The addition of HPO_4^{2-} ions into a freshly prepared aqueous solution containing dissolved $CaCl_2$ at room temperature will cause the immediate precipitation of brushite crystals, provided that the solution pH is between 4 and 6 [28–30]. This is how the brushite powders are readily synthesized in aqueous solutions. However, if one adds H_2PO^{4-} ions into a $CaCl_2$ solution (Ca/P molar = 1 to 2.5) at room temperature, the solution will only be supersatu-

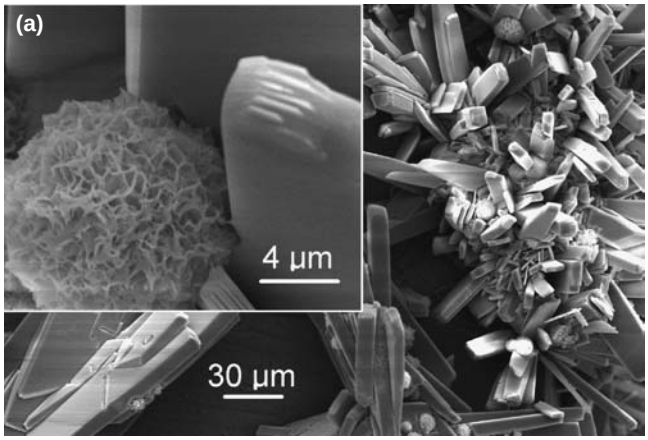

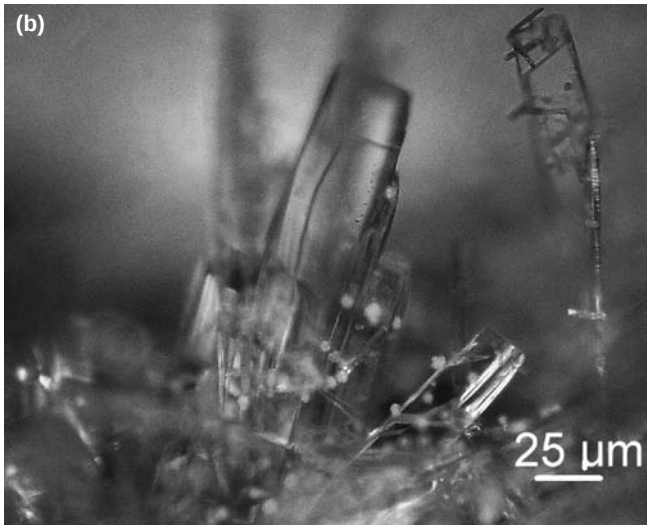

Fig. 5. Morphology of brushite crystals deposited by Solution-3 in 2 h; (a) SEM, (b) optical microscope images.

rated with respect to the formation of brushite, and the solution will be free of precipitates with its pH remaining constant at around 4. Such transparent solutions will require a slight increase in pH (not higher than 6) to nucleate brushite crystals. When the solution pH remains around 4, they will be stable against precipitation. The aforementioned pH increase can be globally accomplished by the addition of $NaHCO_3$ (or via CO_2 gas bubbling). If the substance immersed in such solutions does have a basic surface, then such slight pH increases will be achieved locally.

Therefore, the solutions presented in this work, which were prepared by using $CaCl_2 \cdot 2\,H_2O$ and NaH_2PO_4 to have a Ca/P molar ratio of 2.50, were highly supersaturated with respect to the formation of brushite crystals. Crystallization of brushite from such supersaturated solutions (i. e., solutions 1 and 2) was initiated almost instantaneously upon the insertion of a metallic substrate with a slightly basic surface. The etching of Ti–6Al–4V surfaces by immersing them into NaOH solutions at 60 °C (for 24 h) was extensively described in the previous work of Kokubo et al. [31]. We preferred using the strong base KOH in this study, mainly to prevent the possibility of contaminating the forming brushite crystals with Na^+. Briefly, a basic potassium titanate hydrogel layer with a nanoporous texture (as shown in Fig. 1) was formed on the surface of the substrates after immersion in 5 M KOH solutions at 60 °C for 24 h. Further details of characterization of this hydrogel layer have been described elsewhere [32]. When such KOH-treated substrates were exposed to the solutions disclosed in this study, one may assume the release of K^+ ions via ion exchange with H_3O^+ ion present in the solutions. Such an ion exchange would then form a hydrated titania abundant in Ti–OH groups, which will locally induce a slight increase in the pH value of the solution [31]. This phenomenon triggers the crystallization of CaP on the available surfaces. This also explains why we did not observe a significant amount of brushite formation on unetched Ti–6Al–4V strips.

Solution-1 of this study, which was more dilute in Ca^{2+} and $H_2PO_4^-$ concentrations in comparison to Solution-2, was used to monitor the initial nucleation of nascent brushite crystals on the Ti–6Al–4V strips. On the other hand, Solution-2 was a rapid brushite-depositing solution. The adhesion of these crystals to the titanium alloy surface was somewhat poor and did not even resist the shear stress applied by a fingernail scratch. For that reason, we did not attempt to measure the adhesion strength analytically.

XRD spectra of deposited brushite agreed very well with that presented in ICDD (International Centre for Diffraction Data, Newtown Square, PA) powder diffraction file No. 72-0713. Brushite has a monoclinic (with space group *Ia* and $Z = 4$) unit cell, with the lattice parameters $a = 5.812$ Å, $b = 15.18$ Å, $c = 6.239$ Å, $\beta = 116°25'$, and its crystal structure is closely related to that of gypsum, $CaSO_4 \cdot 2\,H_2O$ [33].

Crystalline brushite bundles and star-like crystals of a unique morphology were observed to form (Figs. 2 and 3), starting from the very early stages of deposition in the solutions of this study. These bundles seemed to originate first from a longitudinally deposited lath-like brushite crystal (Fig. 2 inset), and then continued to grow towards the solution side, following the upwards concentration gradient. The formation and growth pattern of these bundles represented a case of heterogeneous crystallization. The surface topography displayed in the micrographs of Fig. 3 hinted at the presence of a large surface area (although we did not measure it) coat layer on top of the Ti–6Al–4V substrate. The rough microtopography on metallic implant surfaces is believed to enhance the adhesion and proliferation of bone-forming osteoblast cells.

Solution-3, presented in Tables 1 and 2, served the purpose of revealing the possibility of simultaneously depositing both brushite platelets [34] and apatitic CaP spherulites (or globules), when the solution pH was deliberately adjusted right at the intersection point (i. e. pH 6.1) of the solubility isotherms of brushite and OCP (octacalcium phosphate, $Ca_8(HPO_4)_2(PO_4)_4 \cdot 5\,H_2O$ or $Ca_8H_2(PO_4)_6 \cdot 5\,H_2O$). At or above pH 6.1, it is known to be extremely difficult, if not impossible, to eliminate those apatitic or OCP-like spherulites or globules [28]. OCP is known to be a thermodynamically metastable in vivo (and in vitro) biomineralization precursor that easily transforms into more stable apatitic CaP [35]. Solubility isotherms, which would also vary as a function of solution concentration and ionic strength, can be calculated and then drawn [36, 37] for all calcium phosphate phases over the axes of log [Ca] (or log [P]) versus pH for a series of solutions that are all saturated with respect to a certain calcium phosphate salt. These isotherms mean that a CaP salt that has a solubility isotherm positioned below that of another salt will be less soluble (and, therefore, more stable) than the other salt. The SEM micrographs of Fig. 5a depict the formation of OCP (or apatitic CaP) spherulites growing at the expense of brushite, in Solution-3, after 2 h soaking of a Ti–6Al–4V strip. The optical micrograph of Fig. 5b, on the other hand, displays the optically transparent nature of the brushite crystals, as well as the attached spherulites, which may either be those of OCP or apatitic CaP. The increase in the pH of Solution-3 was achieved by using NaCl, which also increased its ionic strength with respect to those of Solutions 1 and 2.

Solutions of this study (i. e., Solutions 1 through 3) were, respectively, 22, 48, and 12.1 times more concentrated than the human blood plasma in terms of Ca and P. If the acidity of brushite ever becomes a concern, then it must be noted that brushite can be easily converted into carbonated, apatitic CaP either by soaking in an SBF solution at 37 °C [28] or in a very dilute NaOH or Na_2CO_3 solution at 65 to 70 °C [38].

In most of the powder synthesis routes, brushite crystallizes with a flat, plate- or lath-like morphology, where the interlocking of these discrete plates or laths with one another is typically minimal [39, 40], in contrast to the morphology exhibited by the samples of this study (Figs. 2 and 3). However, Grases et al. [41], while classifying the morphology of the renal calculi and urinary stones in a clinical study, described the characteristic morphology of brushite crystals to be formed in vivo as flower- or bundle-like, i. e., petal- or lath-like plates originating from one point and opening upwards.

5. Conclusions

Highly concentrated and transparent CaP solutions were developed and used for electroless, solution-based deposition of brushite crystals on Ti–6Al–4V strips at room temperature. The inorganic solutions developed in this study had

Ca^{2+} and HPO_4^{2-} concentrations 12.1, 22, or 48 times that of the human blood plasma. The deposition process was quite robust, and it only required the room temperature immersion of KOH-etched Ti–6Al–4V strips into solutions with pH values ranging from 4.7 to 6.15 for 24 to 72 h. Surfaces of the metal strips were completely covered by brushite crystals which were radiating outwards from the surface.

The author is cordially grateful to Mr. Sahil Jalota and Dr. Sarit B. Bhaduri for their generous help with the characterization runs.

References

[1] L. Winand: Ann. Chim. 6 (1961) 941.
[2] Y.E. Greish, P.W. Brown: J. Biomed. Mater. Res. Appl. Biomat. B 67 (2003) 632.
[3] R.Z. LeGeros, J.P. LeGeros, in: L.L. Hench, J. Wilson (Eds.), An Introduction to Bioceramics, World Scientific Publishing Co, London (1993) 144.
[4] Y.T. Wu, M.J. Glimcher, C. Rey, J.L. Ackerman: J. Mol. Biol. 244 (1994) 423.
[5] C.K. Loong, C. Rey, L.T. Kuhn, C. Combes, Y. Wu, S.H. Chen, M.J. Glimcher: Bone 26 (2000) 599.
[6] T. Kokubo: Acta Mater. 46 (1998) 2519.
[7] G.L. Lange, K. Donath: Biomaterials 10 (1989) 121.
[8] C.Y. Yang, R.M. Lin, B.C. Wang, T.M. Lee, E. Chang, Y.S. Hang, P.Q. Chen: J. Biomed. Mater. Res. 37 (1997) 335.
[9] M. Yoshinari, T. Hayakawa, J.G.C. Wolke, K. Nemoto, J.A. Jansen: J. Biomed. Mater. Res. 37 (1997) 60.
[10] W. Weng, J.L. Baptista: Biomaterials 19 (1998) 125.
[11] L. Tuantuan, J. Lee, T. Kobayashi, H. Aoki: J. Mater. Sci. Mater. M. 7 (1996) 355.
[12] B. Mavis, A.C. Tas: J. Am. Ceram. Soc. 83 (2000) 989.
[13] S. Ban, S. Maruno: J. Biomed. Mater. Res. 42 (1998) 387.
[14] S. Rossler, A. Sewing, M. Stolzel, R. Born, D. Scharnweber, M. Dard, H. Worch: J. Biomed. Mater. Res. 64 (2002) 655.
[15] S. Lin, R.Z. LeGeros, J.P. LeGeros: J. Biomed. Mater. Res. 66 (2003) 819.
[16] M. Shirkhanzadeh, S. Sims: J. Mater. Sci. Mater. M 8 (1997) 595.
[17] M. Kumar, J. Xie, K. Chittur, C. Riley: Biomaterials 20 (1999) 1389.
[18] M.H.P. Da Silva, J.H.C. Lima, G.A. Soares, C.N. Elias, M.C. de Andrade, S.M. Best, I.R. Gibson: Surf. Coat. Tech. 137 (2001) 270.
[19] X. Hou, X. Liu, J. Xu, J. Shen, X. Liu: Mater. Lett. 50 (2001) 103.
[20] J. Redepenning, G. Venkataraman, J. Chen, N. Stafford: J. Biomed. Mater. Res. 66 (2003) 411.
[21] X. Cheng, M. Filiaggi, S.G. Roscoe: Biomaterials 25 (2004) 5395.
[22] S.H. Wang, W.J. Shih, W.L. Li, M.H. Hon, M.C. Wang: J. Eur. Ceram. Soc. 25 (2005) 3287.
[23] B.R. Constantz, B.M. Barr, I.C. Ison, M.T. Fulmer, J. Baker, L. McKinney, S.B. Goodman, S. Gunasekaren, D.C. Delaney, J. Ross, R.D. Poser: J. Biomed. Mater. Res. 43 (1998) 451.
[24] D.D. Lee, A. Tofighi, M. Aiolova, P. Chakravarthy, A. Catalano, A. Majahad, D. Knaack: Clin. Orthop. 367 (1999) 396.
[25] B. Flautre, C. Maynou, J. Lemaitre, P. van Landuyt, P. Hardouin: J. Biomed. Mat. Res. Appl. Biomat. 63 (2002) 413.
[26] R. Tang, M. Hass, W. Wu, S. Gulde, G.H. Nancollas: J. Coll. Int. Sci. 260 (2003) 379.
[27] D. Bayraktar, A.C. Tas: J. Eur. Ceram. Soc. 19 (1999) 2573.
[28] A.C. Tas, S.B. Bhaduri: J. Am. Ceram. Soc. 87 (2004) 2195.
[29] G.H. Nancollas: Adv. Coll. Int. Sci. 10 (1979) 215.
[30] F. Abbona, F. Christensson, M. Franchini-Angela, H.E.L. Madsen: J. Cryst. Growth 131 (1993) 331.
[31] H.M. Kim, H. Takadama, F. Miyaji, T. Kokubo, S. Nishiguchi, T. Nakamura: J. Mater. Sci. Mater. M 11 (2000) 555.
[32] A.C. Tas, S.B. Bhaduri: J. Mater. Res. 19 (2004) 2742.
[33] N.A. Curry, D.W. Jones: J. Chem. Soc. A 1971 (1971) 3725.
[34] A.C. Tas: US Patent No. 6,929,692 August 16, 2005.
[35] M. Iijima, in: L.C. Chow, E.D. Eanes (Eds.), Octacalcium Phosphate. Monogr. Oral Sci. Karger, Basel (2001), Vol. 18, p. 17.
[36] L.C. Chow, S. Takagi: US Patent No: 5,525,148. June 11, 1996.
[37] C. Combes, M. Freche, C. Rey, B. Biscans: J. Mater. Sci. Mater. M. 10 (1999) 231.
[38] R. Rohanizadeh, R.Z. LeGeros, M. Harsono, A. Bendavid: J. Biomed. Mater. Res. A 72 (2005) 428.
[39] S.M. Arifuzzaman, S. Rohani: J. Cryst. Growth 267 (2004) 624.
[40] R. Tang, C.A. Orme, G.H. Nancollas: J. Phys. Chem. B 107 (2003) 10653.
[41] F. Grases, A. Costa-Bauza, M. Ramis, V. Montesinos, A. Conte: Clinica Chim. Acta 322 (2002) 29.

(Received September 30, 2005; accepted February 8, 2006)

Correspondence address

Dr. A. Cuneyt Tas
2. Cadde, 25. Sokak
No: 21
Batikent
Ankara 06370
Turkey
Tel.: 90 312 250 7563
E-mail: c_tas@hotmail.com